Acta Geotechnica (2014) 9:789–798
DOI 10.1007/s11440-014-0345-9

RESEARCH PAPER

Rain-triggered slope failure of the railway embankment at Malda, India

Monal Raj · Aniruddha Sengupta

Received: 9 July 2013 / Accepted: 24 June 2014 / Published online: 6 August 2014

Abstract The common slope stability analysis is incapable of accurately forecasting shallow slides where suction pressures play a critical role. This realization is used for elaborate stability analyses which include soil suction to better predict rainfall-induced slides at railway embankment at Malda where three known cases of slope failures and train derailments occurred after heavy rainfall. The relationship between the soil–water content and the matric suction is established for the embankment soil. It is then used in the coupled analyses of seepage and slope stability to estimate performances of the embankment at different intensity and duration of rainfall. The numerical simulations are performed with the FE code Geo-Studio. The numerical results show significant reduction in the factor of safety of the railway embankment with the increase in the intensity and duration of rainfall. The effectiveness of the proposed mitigation measures including placement of 2 m-wide free draining rockfill across the slopes and drilling 5-m-long sheet pile wall at the toe of the embankment is studied numerically. The study confirms that the proposed mitigation measures effectively increase the factor of safety of the embankment and stabilizing it even in case of a heavy rainfall of 25 mm/h over 12 h.

Keywords Matric suction · Railway embankment · Rainfall-induced landslide · SWCC · Unsaturated soil mechanics

M. Raj · A. Sengupta (✉)
Indian Institute of Technology Kharagpur, Kharagpur 721302, India
e-mail: sengupta@civil.iitkgp.ernet.in

1 Introduction

Failure of natural and man-made slopes is very common in many parts of the world. Depending upon the location, it often leads to major disaster. Slope failure is often caused by steepness of the slope, inadequate strength of the slope materials, deforestation, etc. But rainfall is recognized to be the most common triggering factor for this kind of disaster, especially in tropical regions with hot and humid climatic conditions [5, 26]. Rainwater infiltrates into the unsaturated zone of soil slope and decreases matric suction, and consequently the shear strength of the soil, causing slope failures [4, 6–8, 16, 22, 27, 28, 33, 34, 36, 38, 39]. The characterization of the unsaturated soil is primarily based upon developing a relationship between soil's (total) suction, Ψ, and the gravimetric water content which is termed as the soil–water characteristic curve, SWCC [12]. The total soil suction, Ψ, is the sum of matric suction, Ψ_m, and the osmotic suction, Ψ_o [21]. The matric suction, Ψ_m, is attributed to the interactive adsorbed and capillary forces between water and the soil matric, where as Ψ_o results from the solutes present in the pore solution [14]. Although a number of relationships between rainfall and slope failures can be found in the literature, there have been some debates about the relative role of antecedent rainfall [3, 35]. Antecedent rainfall is the rain that falls in the days immediately preceding a slope failure event. Most or all of the potential slip surfaces may lie initially above the ground water table where the soil is unsaturated with negative pore-water pressure. As the rainwater infiltrates the embankment, the effective stresses within the embankment start to reduce with the decrease in suction pressures in the soil pores and buildup of positive pore pressures until the embankment fails. Surface sloughing commonly occurs on slopes following prolonged period of

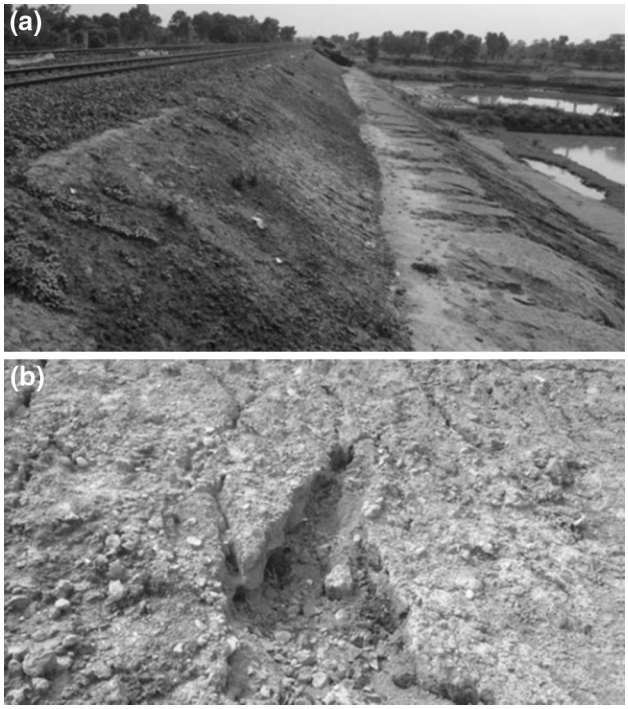

Fig. 1 **a** Railway embankment at the accident site, **b** gully formation on the embankment slope due to seepage of rainwater

precipitation. These failures have received little attention from an analytical standpoint. One of the main difficulties appears to have been associated with the assessment of existing suction pressure and buildup of pore-water pressure with rainwater infiltration into the embankment or slope. It appears that an understanding of unsaturated soil behavior is imperative in formulating a correct analytical solution to the problem.

The repeated failure of the railway embankment at a place called Malda in the state of West Bengal in India is the main focus of the present study. At least three major train accidents have occurred in the recent past at this place causing loss of property and human life. In all the cases, the accidents occurred after continuous heavy rainfall. The investigating agencies have blamed them on the sudden subsidence of the embankment due to pore-water pressure buildup within the embankment and its foundation [30, 32]. Figure 1a shows a portion of the existing railway embankment at the accident site. The site inspection in August 2012 by the authors revealed several gullies and wet areas on the slope of the embankment formed by the seepage of the rainwater. Figure 1b shows one such rainwater gully on the slope near the accident site. Considering the destructiveness of these sudden slope failures, it is decided to perform numerical modeling of the slope failure mechanisms occurring within the embankment to assess the effect of rainfall on the embankment and to estimate the hazard due to sudden subsidence. This kind of slope failure

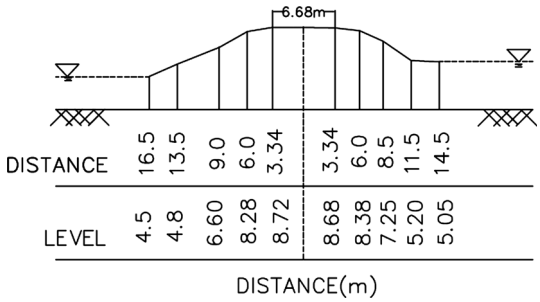

Fig. 2 Cross-sectional profile of the embankment at the accident site

after prolonged and/or heavy rainfall is not very uncommon throughout the world, and several cases have been reported in the literature [1, 6, 9, 29]. But only a very few solutions have been proposed at present on the topic.

2 The study site

2.1 Rainfall at Malda

The climate of Malda is very hot and sultry during the summer season which extends from March to May. The rainy season starts in the middle of June with the coming of southwest monsoons and continues till the middle of September. The month of October and first half of November constitute the post-monsoon season. The Malda region gets about 2,000–4,000 mm rainfall per year [15] and most of the precipitation occurs during the rainy season (June–August). The historical (between 1961 and 2013) maximum intensity of rainfall of 23.75 mm/h was recorded at Malda on September 28, 1995 [17].

2.2 Cross-sectional profile of the embankment

The surveyed profile and the cross-section of the typical railway embankment at Malda, which is chosen for this study, are shown in Fig. 2. The maximum height of the embankment is 4.4 m. The average side slopes of the embankment are 2(H):1(V). The average width of the crest is 6.7 m. The railway embankments at Malda are designed for 25t single axle load from the railway locomotives which are acting on both lines (up and down lines) located on top of it. This results in a 94.5 kPa distributed load on the crest of the embankment. The above distributed load includes a 30 % increase of the actual load to account for a sudden impact. This is in line with the requirements of the Indian Railways [31]. At several locations along the embankment, shallow ponds exist about 1.5–2 m from the toe on both sides of the embankment. One of the common recommendations made by the investigating team after every accident was to fill up these ponds. The soils for the

embankment construction were obtained from the adjacent areas. These excavated areas on both sides of the embankment were fed by rainwater and turned into ponds. These ponds are presently utilized by the local people for the cultivation of fishes. Thus, due to the objection of the local people and due to issues related to environment protection, filling up these ponds are not possible.

2.3 Soil stratification

A total of three boreholes are drilled through the existing embankment at the accident sites. All the boreholes are 15 m deep. Standard penetration tests (SPTs), undisturbed tube sampling and visual characterization of the soil are performed during the drillings. Loose samples are also collected from 1 m depth of the existing embankments for testing and characterization purposes. The borehole logs indicate that the top 9 m of the foundation soil is silty clay of medium consistency. The average SPT blow count (N value) for this layer is between 4 and 5. The undrained shear strength is typically between 25 and 50 kPa. Below 9 m, the soil is silty clay with stiff consistency. Traces of fine sand are visible at places. The SPT blow count increases to 10–15 for this layer. Typical undrained shear strength for this layer is found to be between 50 and 100 kPa.

3 Properties of the soil

Standard laboratory tests are performed to determine the properties and classification of the soil. The laboratory-specific gravity tests indicate that the soil has a specific gravity of 2.66. The shear strengths of the soil are obtained from conventional drained direct shear tests. The tests show that the soil has cohesion (c') of 0.2 kPa and an effective internal angle of friction (ϕ') of 29.5°.

3.1 Grain size distribution of the soil

The grain size distribution of the embankment and top 6 m of the Malda soil is shown in Fig. 3. The embankment and the top 6 m of the soil contain 18 % sand, 81 % silt and 1 % clay. The liquid limit and plasticity index of the soil are 27.5 and 3.6, respectively. The UCSC classification of the embankment and the top 6 m Malda soil is CL (clay with low plasticity).

3.2 Soil–water characteristics curve (SWCC)

The soil–water characteristic curve for the Malda soil is determined by following the standard test method [2, 25] using tensiometers. The soil was first dried and then known amount of water is added to it. And every time, the corresponding suction force measured by a tensiometer is noted down. The procedure is repeated for different water content of the soil. Figure 4 shows the SWCC curve for the embankment and the top 6 m of the Malda soil.

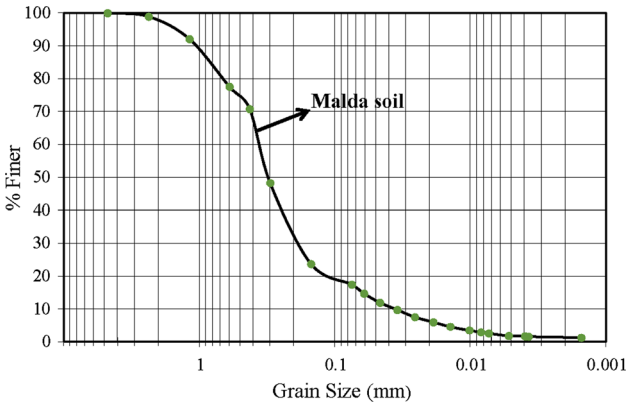

Fig. 3 Grain size distribution of the embankment soils

3.3 Variation of hydraulic conductivity with suction

The saturated hydraulic conductivity k_s obtained from falling head permeability tests is 8.4×10^{-4} cm/s. This value is further used to establish a relationship between hydraulic conductivity and suction empirically using Van Genuchten method [37]. Figure 4 shows the variation of hydraulic conductivity with the suction pressure for the Malda soil.

4 Numerical analysis

The stability of the typical embankment cross-section at Malda is numerically evaluated by a commercial finite

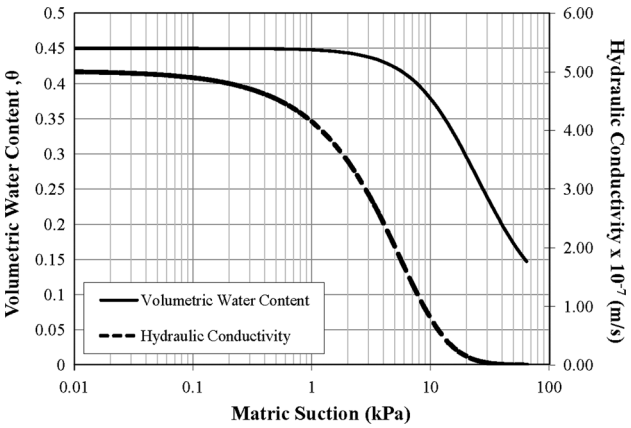

Fig. 4 Variation of volumetric water content and hydraulic conductivity with suction pressures for the Malda soil

element software called GEO-STUDIO 2007 [13]. The program has seven modules. Out of the seven, the first three modules called SEEP/W [18], SLOPE/W [19] and SIGMA/W [20] are utilized to study the behavior of the Malda embankment. A plane strain condition is assumed for all the analyses. The soil embankment is discretized in the numerical analyses by standard two-dimensional quadrilateral and triangular elements. A uniformly distributed load of 94.5 kN/m on the crest of the embankment due to locomotives on both up and down lines has been also considered in the stability analyses of the embankment.

Before the stability analyses of the embankment, the initial conditions of the pore-water pressures are obtained by transient seepage analysis using the SEEP/W program. The result of the transient analysis is then imported into the stability analysis model. The negative pore-water pressure distribution within the embankment is computed under a given intensity and duration of rainfall. Before the transient seepage analysis is carried out, a steady state analysis is done to achieve a hydrostatic condition within the embankment and the foundation. In the transient analyses, the infiltration rate is determined by dividing the amount of rainfall in an event by the total duration of the rainfall event and applied to the slope boundary as a surface flux. The transient analysis is carried out for different infiltration rate and results are recorded at 2.4-h interval.

The transient analysis program, SEEP/W, is formulated on the basis that the flow of water through both saturated and unsaturated soil follows Darcy's law which states that:

$$q = ki \tag{1}$$

where q the specific discharge, k the hydraulic conductivity and i the gradient of total hydraulic head.

The Darcy's law is also applied to the flow of water through unsaturated media. The only difference is that under the unsaturated flow condition, the hydraulic conductivity is no longer a constant, but varies with changes in the water content and indirectly varies with changes in the pore-water pressure.

The general governing differential equation for two-dimensional seepage is expressed as:

$$\frac{\partial}{\partial x}\left(k_x \frac{\partial H}{\partial x}\right) + \frac{\partial}{\partial y}\left(k_y \frac{\partial H}{\partial y}\right) + Q = \frac{\partial V}{\partial t} \tag{2}$$

where H total head, k_x, k_y hydraulic conductivity in the x and y directions, Q applied boundary flux, V volumetric water content and t time.

This equation states that the difference between the flow (flux) entering and leaving an elemental volume at a point in time is equal to the change in the storage of the soil media. More fundamentally, it states that the sum of the rates of change of flows in the x and y directions plus the external applied flux is equal to the rate of change of the volumetric water content with respect to time.

The program is formulated for conditions of constant total stress (σ); that is, there is no loading or unloading of the soil mass. It also assumes that the pore-air pressure, u_a, remains constant at atmospheric pressure during transient processes. This means that $(\sigma - u_a)$remains constant and has no effect on the change in volumetric water content. The changes in volumetric water content are consequently dependent only on the changes in the $(u_a - u_w)$ stress state variable, and with u_a remaining constant, the change in volumetric water content is a function of only the pore-water pressure (u_w) changes. As a result, the governing differential equation (Eq. 2) used in the SEEP/W finite element formulation reduces to the following:

$$\frac{\partial}{\partial x}\left(k_x \frac{\partial H}{\partial x}\right) + \frac{\partial}{\partial y}\left(k_y \frac{\partial H}{\partial y}\right) + Q = m_w \gamma_w \frac{\partial H}{\partial t} \tag{3}$$

where m_w and γ_w are the slope of the storage curve and unit weight of water.

The SLOPE/W program considers unsaturated shear strength conditions when the suction pressures exist or the pore-water pressures are negative. The Geostudio program offers two ways to model the increase in shear strength due to the soil suction.

In the first option, ϕ^b, an angle defining the increase in strength due to the negative pore-water pressure is used to compute the mobilized shear force at the base of a slice. The SLOPE/W program implemented the following equation for the shear stress, τ, proposed by Krahn and Fredlund [21], Fredlund et al. [10] and Fredlund and Rahardjo [11]).

$$\tau = c' + (\sigma_n - u_a)\tan\phi' + (u_a - u_w)\tan\phi^b \tag{4}$$

where c' effective cohesion of the soil, σ_n normal stress, u_a pore-air pressure, u_w pore-water pressure, ϕ' effective friction angle of the soil and ϕ^b an angle defining the increase in strength due to the negative pore-water pressure. For practical purposes, ϕ^b can be taken as $\phi'/2$.

In the above equation, ϕ^b is treated as a constant value, but in reality, this parameter varies with the degree of saturation as given by Lu et al. [23, 24]. In the capillary zone where the soil is saturated, but the pore-water pressure is under tension, ϕ^b is equal to the effective friction angle φ'. As the soil becomes unsaturated, φ^b decreases. The decrease in ϕ^b is a reflection of the fact that the negative pore-water pressure acts over a smaller area. More specifically, ϕ^b is related to the soil–water characteristic (SWCC) curve.

In the second alternative, the following equation for the shear stress as proposed by Vanapalli et al. [36] based on soil–water characteristics curve is utilized.

$$\tau = c' + (\sigma_n - u_a)\tan\phi' + (u_a - u_w)\left[\left(\frac{\theta_w - \theta_r}{\theta_s - \theta_r}\right)\tan\phi'\right] \quad (5)$$

In the above equation, θ_w is the volumetric water content, θ_s is the saturated volumetric water content and θ_r is the volumetric water content at residual condition. When the water content is at saturation ($\theta_w = \theta_s$), 100 % of the suction contributes to the strength. When the water content is at the residual value ($\theta_w = \theta_r$), the suction makes no contribution to the strength. Thus, the water content function is used in essence to apportion the suction contribution to the strength.

The above alternative (Eq. 5) is used in the present analyses for the computation of the stresses. The above equation is similar to that proposed by Lu et al. [23, 24].

The factor of safety is then calculated by

$$FS = \frac{\sum \tau_r}{\sum \tau_m} \quad (6)$$

where $\Sigma\tau_r$ is the summation of the resisting shear stresses computed from Mohr–Coulomb equation and corresponding material parameters. $\Sigma\tau_m$ is the summation of the mobilized shear stresses.

The slope stability analysis is performed using four well-known limit equilibrium methods, that is, Morgenstern and Price method, Janbu's method, ordinary method of slice and Bishop's simplified method [13]. Above limit equilibrium methods are different in how they are handling the four inter-slice forces to make the equilibrium equations determinate. The Morgenstern and Price method allows one to define the relationship between the inter-slice forces and satisfies both the force and the moment equilibrium equations. The Janbu's simplified method assumes the inter-slice forces to be horizontal and satisfies the force equilibrium equations only. The ordinary method of slice or Fellenius method assumes no inter-slice forces and satisfies the moment equation only. The Bishop's simplified method assumes the inter-slice forces to be horizontal and satisfies only moment equilibrium condition. In the present analyses, the minimum factor of safety obtained by applying the above four methods is only reported for each case. The material parameters assumed for the slope stability analyses is given in Table 1.

Table 1 Material parameters for Malda embankment soil

Soil property	Value
Dry unit weight (γ_d)	14.5 kN/m^3
Cohesion (c')	0.2 kPa
Friction angle (ϕ')	29.5°
Poisson's ratio	0.25
Young's modulus (E)	4 MPa
Saturated water content (w)	29.55 %
Specific gravity (G)	2.66
Saturated hydraulic conductivity(k_s)	8.4×10^{-6} m/s

5 Results

The results obtained from the numerical analyses of seepage and stability of the actual embankment at Malda is utilized to help understand the water table fluctuation within the embankment during rainy season, loss of suction within the railway embankment due to rainfall infiltration and variation of the factor of safety with rainfall.

5.1 Water table fluctuation and reduction of suction pressure with rainfall duration

The response of water table and the reduction of the suction pressures within the actual Malda railway embankment to different rainfall intensities are studied numerically. The rainfall intensities considered in this study are 2, 4, 8, 16, 25, and 32 mm/h. For each case, the rainfall infiltration rate is computed from the rainfall intensity and the duration of the rainfall, and applied as a boundary flux across the slope.

Figure 5 shows the distribution of the suction pressures and the pore-water pressures within the Malda embankment for the case of 8 mm/h intensity of rainfall at the end of 2.4, 7.2 and 17 h. The figures demonstrate how the suction pressures diminish and pore-water pressures increase within the railway embankment with the duration of the rainfall.

Figure 6 shows the maximum suction pressure within the embankment for the different intensity and the different duration of rainfall. For 2, 4 and 8 mm/h rainfall, significant suction pressures remain in the embankment even after 24 h of rainfall. For the case of 16 mm/h rainfall, the suction pressures disappear after 18 h of rainfall. For 25 mm/h and 32 mm/h rainfall, it disappears after 13 and 10 h of rainfall, respectively.

5.2 Stability analysis of the embankment

The slope stability analyses of the Malda embankment is analyzed after each rainfall event by considering the suction pressures and pore-water pressures within the embankment obtained from the above seepage analyses. The factor of safety against sliding reported here for each case is the lowest factor of safety obtained by applying the different limit equilibrium methods mentioned in Sect. 4.

Indian Railways [31] requires a minimum factor of safety of 1.4 for sliding stability under normal long-term

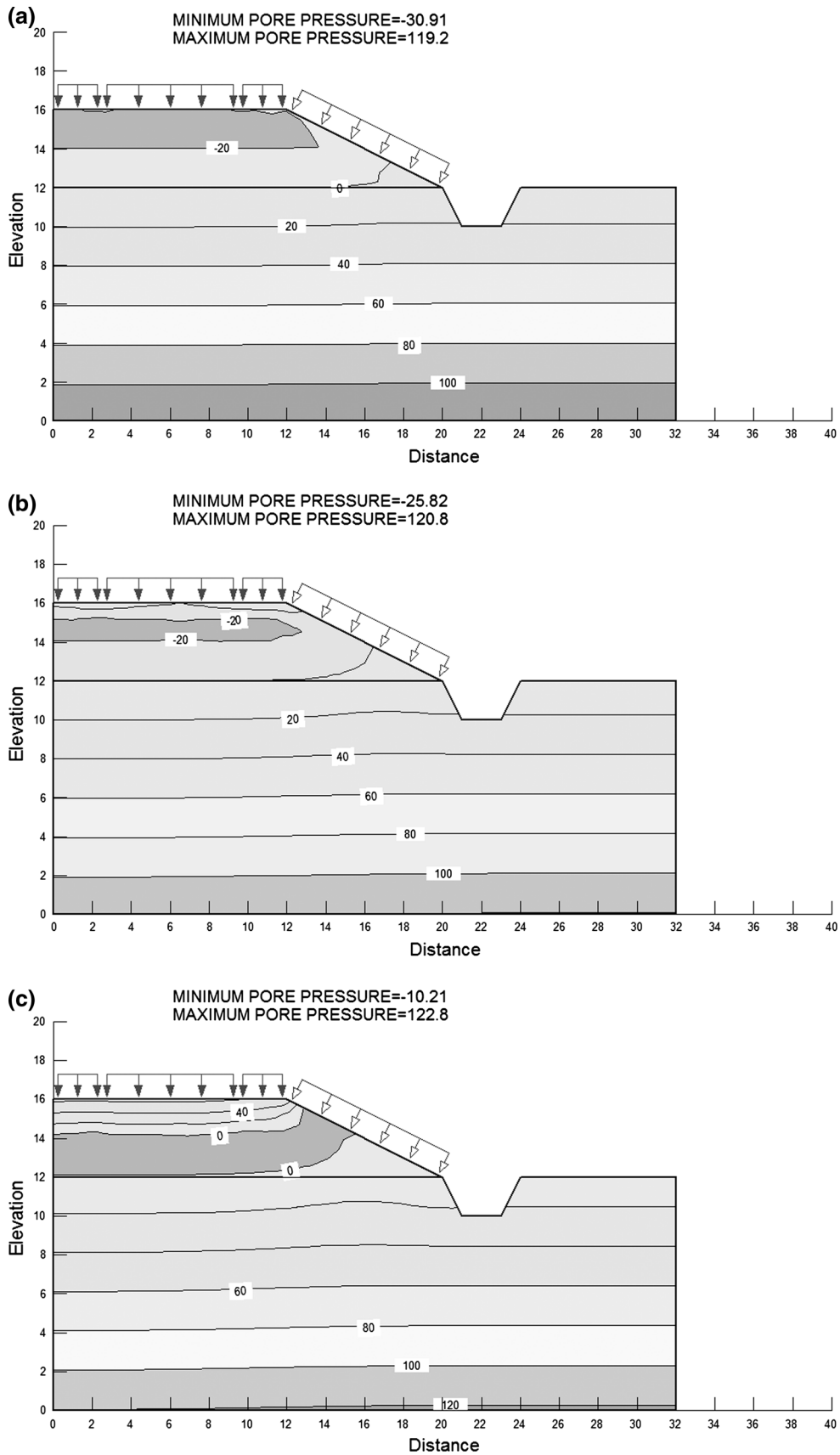

Fig. 5 Distribution of suction and pore-water pressure for 16 mm/h rainfall after **a** 2.4 h, **b** 7.2 h, and **c** 17 h

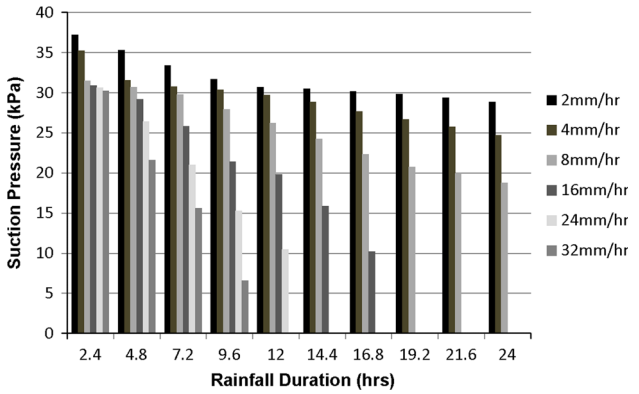

Fig. 6 Reduction in suction pressure within the Malda embankment due to rainfall

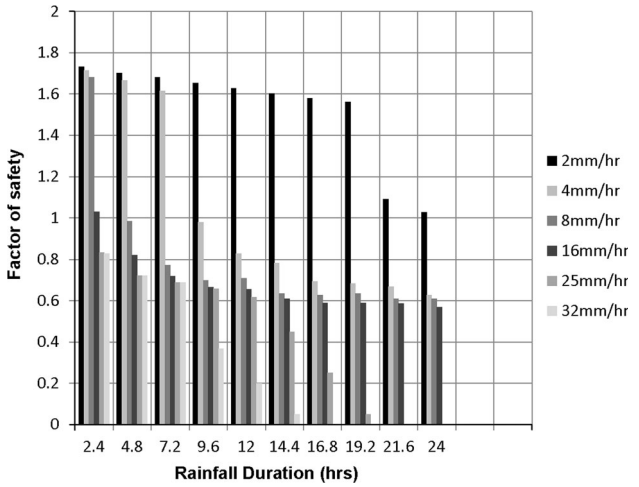

Fig. 7 Reduction in factor of safety of the Malda embankment due to rainfall

(steady state) condition of an embankment of height 4 m and above. For transient condition like high water table (flood) condition, a factor of safety of 1.2 is considered to be sufficient.

For the normal long-term condition, that is, when the ground water table is at and below the toe of the Malda embankment, the computed factor of safety is 1.8. The critical slip surface for this case obtained after detailed search procedure is shown in Fig. 8. This factor of safety is well above the minimum required factor of safety. Figure 7 summarizes the theoretical factor of safety of the Malda embankment against sliding for different intensity and different duration of rainfall. As may be seen from the figure, for 2 mm/h rainfall, the embankment satisfies stability criteria even when the duration of rainfall is 20 h. However, the factor of safety drops rapidly if the duration of rainfall exceeds 20 h. The embankment remains stable theoretically for 8 h of 4 mm/h rainfall. Beyond 8 h of

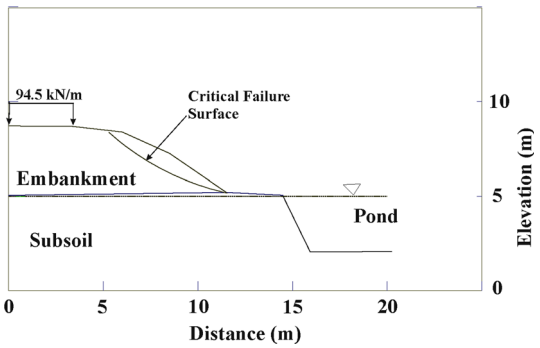

Fig. 8 Critical slip surface within the Malda embankment from numerical analyses

rainfall, its factor of safety drops drastically. Similarly, for 8 mm/h rainfall, the embankment remains stable only if the duration of the rainfall is 3 h. The results also indicate that if the rainfall is more than 8 mm/h, the embankment will not be stable. Since very little record on rainfall at Malda in terms of intensity and duration of the rainfall is available for the date when embankment collapsed in July 2011, nothing could be said with confidence how much rainfall triggered the collapse of the embankment. But the present results confirm that an overnight rainfall of 4 mm/h or more could trigger a collapse of the Malda railway embankment. As discussed before, this much of rainfall is not unusual for the Malda region during the months of June, July and August.

6 Remedial measures

The limit equilibrium analyses of the existing embankment slope indicate that in dry condition, the slope has adequate factor of safety. But when the existing suction pressures go down and pore-water pressures within embankment build up as happening during rainy season, the factor of safety of the slope becomes inadequate. The present analyses indicate that the embankment and the top foundation materials are silty in nature and have very low shear strengths. They are also prone to erosion and piping. Several gullies are noticed on the sides of the embankment during the field visits. During and after prolong rainfall events, as the pore-water pressure starts to rise, the effective stresses within these materials start to drop and the embankment fails all of a sudden. The possible remedial measures should include protection of existing embankment toes, protection of banks of the existing ponds, preventing pore-water pressure buildup within embankments and safe passage of water (or prevention of surface erosion). Several possible modifications of the slope were reviewed before this study. These include flattening of the slopes, putting piles at the

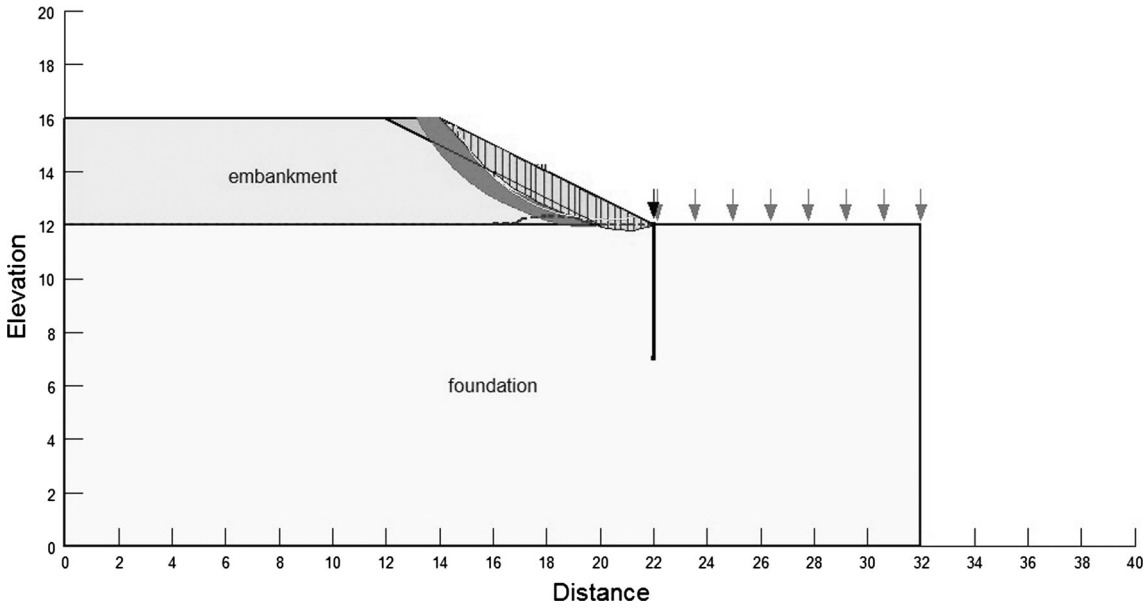

Fig. 9 Critical sip surface within the embankment with rockfill berm and sheet piling in place

embankment toe, putting piles through embankment, installing soil and rockfill berm at the toe. The remedial measures suggested and being implemented at the site include building a rockfill berm, 2 m wide at the toe of the existing embankment and with 2(H):1(V) outer slope on top of a 0.5-m wide stone dust/sand filter layer for the stability of the embankment as well as for the prevention of erosion and gullies during rainy season. A 1-m-wide and 0.5-m-deep filter/drain material (clean sand/stone dust) is also recommended on the crest under the ballast and rockfill at 20 m apart (center to center) to help draining the rainwater and to prevent it infiltrating into the clayey embankment material. The finished surfaces at the crest should have a minimum outward slope of 1 in 20 on both sides. A 5-m-long steel sheet pile wall has been also suggested along the bank of the existing adjacent ponds to protect against cave in.

A study of the suggested remedial measures like putting a rockfill berm (with permeability of order of 10^{-2} m/s) on existing slopes and constructing a sheet pile wall at or near the toes of the embankment are also examined numerically. Figure 9 shows the potential slip surface obtained from the numerical analyses for the Malda embankment with the proposed modifications.

The theoretical factor of safety of the embankment with 1-m-wide rockfill berm on top of the slopes with and without 5-m-long sheet pile at the toe is shown in Fig. 10 for a theoretical case of 25 mm/h rainfall intensity over a duration of 0–12 h. This rainfall intensity and duration considered here are conservative as they exceed the measured historical data on maximum rainfall in Malda region.

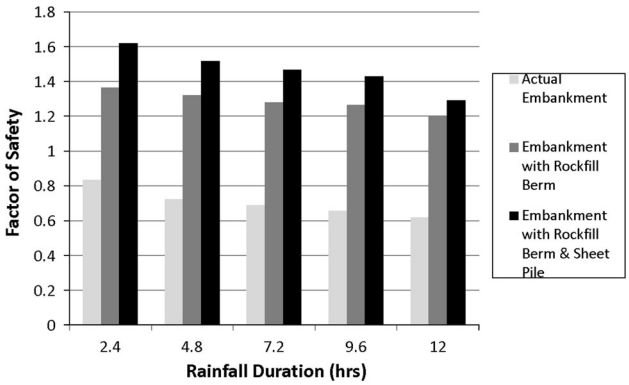

Fig. 10 Factor of safety of the Malda embankment with proposed modifications for 25 mm/h rainfall events

As shown in Fig. 7, the existing embankment will not survive this high intensity of rainfall. However, the safety factor for the modified embankment with 1-m-wide rockfill berm on top of the slopes is found to be adequate (factor of safety >1.2) for 12 h of 25 mm/h rainfall. The numerical analyses show that the embankment near the toes is more susceptible to failure due to a sudden loss in suction pressure and a rapid rise in pore-water pressure in that zone. The sheet piling at the toe of the embankment along with the proposed rockfill berm on the slopes will further enhance the stability of the embankment.

7 Conclusions

The predictions of the numerical analyses show considerable effect of suction pressure on the stability of an

embankment slope. The slope may become potentially unstable with the reduction of the soil suction. During the time of rain infiltration, suction pressure in the soil decreases, and thus, the effective shear strength of a slope reduces, which in turn reduces the factor of safety. The rate of decrease in factor of safety is faster for a soil with higher infiltration rate. It is also observed that placing proper drained material over the slope of the embankment can increase the stability to large extent and also prevent erosion and gully formation, which is a very common problem reported.

The numerical analyses of the railway embankment at Malda show that for 2 mm/h rainfall, the embankment satisfies stability criteria even when the duration of rainfall is 20 h. However, the factor of safety drops rapidly if the duration of rainfall exceeds 20 h. The embankment remains stable theoretically for 8 h of 4 mm/h rainfall. Beyond 8 h of rainfall, its factor of safety drops drastically. Similarly, for 8 mm/h rainfall, the embankment remains stable only if the duration of the rainfall is 3 h. The results also indicate that if the rainfall is more than 8 mm/h, the Malda embankment will not be stable. This possibly explains the derailments that occurred at the site after heavy rainfall.

The theoretical study of the remedial measures suggested for the railway embankment at Malda shows that placing a 2-m-wide free draining rockfill berm on top of the slopes will help stabilizing the embankment even during a 12 h of 25 mm/h rainfall event. The factor of safety of the embankment further enhances if the toes of the embankment are also protected by 5-m-long sheet pile walls.

The hydrological parameters like evaporation, evapotranspiration, depression storage, vegetative cover, surface runoff can also affect the negative pore pressure distribution within an embankment and the overall stability of the embankment. The contributions of these factors are not considered in the present study but may be incorporated in the future.

References

1. Aleotti P (2004) A warning system for rainfall-induced shallow failures. Eng Geol 73(4):247–265
2. ASTM (2004). Standard guide for measuring matric potential in the vadose zone using tensiometers. ASTM standard D3404-91. American Society of Testing materials, West Conshohoken, PA
3. Au SWC (1998) Rain-induced slope instability in Hong Kong. Eng Geol 51(1):1–36
4. Borja RI, Liu X, White JA (2012) Multiphysics hillslope processes triggering landslides. Acta Geotech 7:261–269
5. Brand EW (1992) Keynote paper: slope instability in tropical areas. Proceeding of 6th international symposium on landslides, Rotterdam, Netherlands, pp 2031–2051
6. Cascini L, Cuomo S, Pastor M, Sorbino G (2010) Modeling of rainfall-induced shallow landslides of the flow. J Geotech Geoenviron Eng (ASCE) 136(1):85–98
7. Casini F, Vaunat J, Romero E, Desideri A (2012) Consequences on water retention properties of double-porosity features in a compacted silt. Acta Geotech 7:139–150
8. Fourie AB (1996) Predicting rainfall-induced slope instability. ICE Geotech Eng 119(4):211–218
9. Fowze JSM, Bergado DT, Soralump S, Voottipreux P (2012) Rain-triggered landslide hazards and mitigation measures in Thailand: from research to practice. J Geotext Geomembr 30:50–64
10. Fredlund DG, Morgenstern NR, Widger RA (1978) The shear strength of unsaturated soils. Can Geotech J 15(3):313–321
11. Fredlund DG, Rahardjo H (1993) Soil mechanics for unsaturated soils. Wiley, New York
12. Fredlund DG, Xing A (1994) Equation for soil water characteristic. Can Geotech J 31(3):521–532
13. GEO-SLOPE Intl. Ltd. (2007). Seepage modeling with SEEP/W: an engineering methodology. 2007 edition, GEO-SLOPE Intl. Ltd, Calgary, Alberta, Canada
14. Hillel D (1998) Environmental soil physics. Academic, New York, p 757
15. IMD (2012) Monsoon 2012: a report. IMD MET monograph no. 13/2013, Pai DS, Bhan SC (eds) National Climate Centre, Indian Meteorological Department, Government of India, Pune, India
16. Jordan CA (2011) Combined hydrology and slope stability assessment of Olympic region of Washington State. PhD Dissertation, University of Washington, USA
17. Khaladkar RM, Mahajan PN, Kulkarni JR (2009) Alarming rise in the number and intensity of extreme point rainfall events over the Indian region under climate change scenario. Research report no RR-123, ISSN 0252-1075, Indian Inst. of Tropical Meteorology, Maharashtra, India
18. Krahn J (2008) Seepage modelling with SEEP/W—an engineering methodology, 3rd edn. March 2008, Geo-Slope International Ltd., Calgary, Alberta, Canada
19. Krahn J (2008) Stability modeling with SLOPE/W—an engineering methodology, 3rd edn. March 2008, Geo-Slope International Ltd., Calgary, Alberta, Canada
20. Krahn J (2008) Load deformation with SIGMA/W—an engineering methodology, 3rd edn. March 2008, Geo-Slope International Ltd., Calgary, Alberta, Canada
21. Krahn J, Fredlund DG (1972) On total matric and osmotic suction. J Sci 114(5):339–348
22. Li X, Pei X, Gutierrez M, He S (2012) Optimal location of piles in slope stabilization by limit analysis. Acta Geotech 7:253–259
23. Lu N, Wayllace A, Oh S (2013) Infiltration-induced seasonally reactivated instability of a highway embankment near the Eisenhower tunnel, Colorado, USA. Eng Geol 162:22–32
24. Lu N, Sener-Kaya B, Wayllace A, Godt JW (2012) Analysis of rainfall-induced slope instability using a field of local factor of safety. Water Resour Res 48:W09524. doi:10.1029/2012WR011830
25. Marinho FAM (2005) Nature of soil–water characteristic curve for plastic soils. J Geotech Geoenviron Eng (ASCE) 131(5): 654–661
26. McDougall J, Ng CWW, Shi Q (1999) Discussion of influence of rainfall intensity and duration on slope stability in unsaturated soils. Q J Eng Geol Hydrogeol 32(3):303
27. Meier J, Moser M, Datcheva M, Schanz T (2013) Numerical modeling and inverse parameter estimation of the large-scale mass movement Gradenbach in Carinthia (Austria). Acta Geotech 8:355–371
28. Rahardjo H, Lee TT, Leong EC, Rezaur RB (2005) Response of a residual soil slope to rainfall. Can Geotech J 42(2):340–351

29. Rahimi A, Rahardjo H, Leong C (2011) Effect of antecedent rainfall patterns on rainfall-induced slope failure. J Geotech Geoenviron Eng (ASCE) 137(5):483–491
30. RDSO (2011) Rehabilitation of unstable formation between Gour Malda and Jamirghata Stations, Malda Division, Eastern Railway. Consultancy report no. RDSO/2011/GE:CR-0157, Geotechnical Engineering Directorate, RDSO, Lucknow, India
31. RDSO (2003) Guidelines for Earthwork in Railway Projects. Guidelines no. GE: G-1, Ministry of Railways, Govt. of India, Geotechnical Engineering Directorate, Research Designs and Standards Organization, Lucknow, India
32. RDSO (1998) Rehabilitation of weak formation between Gour Malda and Malda Town on Malda Division Eastern Railway. Consultancy report no: GE-20, Geotechnical Engineering Directorate, RDSO, Lucknow, India
33. Smith PGC (2003) Numerical analysis of infiltration into partially saturated soil slopes. PhD Dissertation, Imperial College of Science, Technology and Medicine, London, UK
34. Stratton, Yee Carlton (1975) Soil and hydrological factors affecting stability of natural slopes in the Oregon Ranges. PhD Dissertation, School of Forestry, Oregon State University Corvallis, USA
35. Ugai K, Cai F (2004) Numerical analysis of rainfall effects on slope stability. Int J Geomech 4(2):69–78
36. Vanapalli SK, Fredlund DG, Pufahl DE, Clifton AW (1996) Model for the prediction of shear strength with respect to soil suction. Can Geotech J 33:379–392
37. Van Genuchten MTh (1980) A closed form equation for predicting the hydraulic conductivity of unsaturated soils. Soil Sci Soc Am J 44:892–898
38. Yoshida Y, Kuwano J, Kuwano R (1991) Rain-induced slope failures caused by reduction in soil strength. Soils Found 31(4):187–193
39. Zou Y (2012) A macroscopic model for predicting the relative hydraulic permeability of unsaturated soils. Acta Geotech 7:129–137